High Strength Concrete Columns Subjected to Earthquake Type Loading

O. Bayrak[1] and S.A. Sheikh[2]

ABSTRACT

This paper presents results from an extensive experimental research program in which large-size confined concrete column specimens (305 x 305 x 1473 mm columns and 508 x 702 x 813 mm stubs) were tested under axial load and cyclic displacement excursions simulating earthquake forces. Unconfined concrete strength varied between 30 MPa and 102 MPa. The focus of this paper is to evaluate the behavior of high strength concrete (HSC) columns in relation to that of normal strength concrete (NSC) specimens. Other major variables that have been included for investigation are steel configuration, amount of confining steel and axial load level. In the light of the test results confinement provisions of the current design codes are critically examined.

INTRODUCTION

The response of framed concrete structures designed according to the current seismic design philosophy, when they are subjected to severe earthquakes, is not expected to be elastic. The ability of a structure to withstand a severe earthquake depends mainly on the formation of plastic hinges and their capacities to absorb and dissipate energy without significant loss of strength. To ensure stability as well as the vertical load carrying capacity while structure undergoes large lateral displacements, "strong column-weak beam" concept is suggested in most design codes (ACI 318-89, CAN3-A23.3M84) so that plastic hinges form in beams rather than in columns. However, structural damage observed during many earthquakes has shown that formation of plastic hinges in columns can not be entirely avoided; therefore the potential plastic hinge regions of columns must be detailed to ensure their ductile behavior which can be achieved by confining concrete effectively. Tests on NSC confinement have recently been reported extensively but data on HSC columns in this area is very limited particularly for tests under high axial load and large inelastic cyclic displacement excursions. Results from five such tests are reported here and compared with those from NSC columns.

EXPERIMENTAL PROGRAM

Each specimen consisted of a 305 x 305 x 1473 mm column and 508 x 762 x 813 mm stub (Figure 1). The column, represented the part of a column in a regular building frame between the section of maximum moment and the point of contraflexure. The stub represented a discontinuity like a beam

---

[1] Graduate Student, Department of Civil Engineering, University of Toronto, Toronto, Ontario, M5S 1A4
[2] Professor, Department of Civil Engineering, University of Toronto, Toronto, Ontario, M5S 1A4

column joint or a footing. Table 1 gives the details of the specimens tested in the current phase ($f_c' >$ 70 MPa) and some of the specimens tested earlier ($f_c' \approx 30$ MPa) (Sheikh and Khɔury 1993). The first letter in specimen designations refers to the steel configurations shown in Table 1.

Table 1. Details of the Test Specimens

Specimen	f_c'	Lateral Steel				Longitudinal Steel				P
	(MPa)	Size (mm)	Spacing (mm)	ρ_s (%)	f_{yh} (MPa)	No.of Bars	Size (mm)	ρ_t (%)	f_{yl} (MPa)	$\overline{P_o}$
ES-1HT	72.1	16.0	95	3.15	463	8	19.5	2.58	454	0.50
AS-2HT	71.7	11.3	90	2.84	542	8	19.5	2.58	454	0.36
AS-3HT	71.8	11.3	90	2.84	542	8	19.5	2.58	454	0.50
AS-5HT	101.8	11.3 16.0	90 90	4.02	542 463	8	19.5	2.58	454	0.48
ES-8HT	102.2	16.0	70	4.29	463	8	19.5	2.58	454	0.50
ES-13	32.5	12.7	114	1.69	464	8	19	2.44	507	0.63
AS-17	31.3	9.5	108	1.68	507	8	19	2.44	507	0.63

Each specimen was tested under a constant axial load and reversed cyclic lateral displacement excursions until it was unable to maintain the axial load. The lateral load was applied at the stub near the stub-column interface (Figure 1) thus the column test region near the stub was subjected to constant axial force and cyclic moment and shear. The first displacement cycle peaked at 75% of the elastic or yield displacement (Δ_1), which can be defined as the lateral deflection corresponding to the estimated lateral load capacity (P_{max}) on a straight line joining origin and a point about 65% of P_{max} on the lateral load-displacement curve. It should be recognized that both Δ_1 and P_{max} were calculated using the theoretical sectional response of the column and integrating curvatures along the length of the specimen. Subsequent displacement excursions consisted of two cycles each at Δ_1, $2\Delta_1$, $3\Delta_1$ and so on.

RESULTS

All specimens except AS-2HT were loaded downward first (Figure 1). First signs of distress in all the tested specimens were the cracks in the top and bottom concrete cover. Both the number of cracks formed and their lengths increased in the first three cycles as the number of displacement excursions to which specimens were subjected to, increased. For most specimens, it was in the first peak of the fourth cycle ($\Delta=2\Delta_1$) that the top concrete cover spalled suddenly, and the bottom concrete cover spalled in the

478

next cycle. Closely spaced ties formed a weak plane between the concrete core and the cover and accelerated the spalling of concrete cover.

Figure 2 illustrates the definitions of section ductility parameters used to evaluate the performances of the specimens. Using these parameters the effects of different variables such as the level of axial load, steel configuration and concrete strength on the behavior of HSC columns are evaluated.

Effect of axial load: Specimens AS-2HT and AS-3HT are very similar in every respect except that P/P_o is 0.36 for Specimen AS-2HT and it is 0.50 for Specimen AS-3HT. Moment-curvature relationships of the failed sections of the specimens AS-2HT and AS-3HT are provided in Figure 3. Theoretical section moment capacity M_i shown in the figure was obtained using stress-strain curve of unconfined concrete. Table 2 shows the section ductility parameters.

Table 2. Section Ductility Parameters

Specimen	f_c' (MPa)	Lateral Steel		Axial Load	Curvature Ductility Factor		Cumulative Curvature Ductility Ratios		Energy Damage Indicators	
		ρ_s (%)	$\dfrac{A_{sh}}{A_{sh(ACI)}}$	$\dfrac{P}{P_o}$	μ_ϕ @		$N_{\phi 80}$	$N_{\phi t}$	E_{80}	E_t
					$0.8M_{max}$	$0.9M_{max}$				
ES-1HT	72.1	3.15	1.13	0.50	6.6	5.9	19	25	80	105
AS-2HT	71.7	2.84	1.19	0.36	15.8	13.6	53	113	631	1412
AS-3HT	71.8	2.84	1.19	0.50	10.1	9.1	20	42	161	396
AS-5HT	101.8	4.02	1.09	0.48	9.6	5.6	27	49	144	311
ES-8HT	102.2	4.29	1.08	0.50	6.7	5.1	14	22	33	99
ES-13	32.5	1.69	1.34	0.63	6.0	2.5	15	26	53	110
AS-17	31.3	1.68	1.52	0.63	12.0	10.5	52	58	402	443

An increase in the axial load from $0.36P_o$ to $0.50P_o$ caused significant decreases in all section ductility parameters similar to what has been observed in NSC columns (Sheikh and Khoury 1993). Reductions of 36%, 62% and 74% were observed in curvature ductility factor $\mu_{\phi 80}$, cumulative curvature ductility ratio $N_{\phi 80}$ and energy damage indicator E_{80}, respectively. A higher axial load level resulted in an increase in the rate of stiffness degradation with every load cycle and adversely affected the cyclic performance of HSC columns. These results underlined the need to take into account the level of axial load when computing the required amount of transverse steel.

Effect of steel configuration: Specimens ES-1HT and AS-3HT, respectively, contained 13% and 19% more transverse steel than ACI 318-89 requirements and were tested under the same level of axial load. In ES-1HT only four corner longitudinal bars were supported by tie bends and in AS-3HT all the

479

longitudinal bars were laterally supported by tie bends (see sketches in Table 1). Moment-curvature relationships of the failed sections of the Specimens ES-1HT and AS-3HT in Figure 3 and section ductility parameters in Table 2 illustrate the effect of steel configuration on column behavior.

Curvature ductility factors, $\mu_{\phi 80}$ and $\mu_{\phi t}$, of Specimen AS-3HT are approximately 50% larger than those of ES-1HT and similarly cumulative curvature ductility ratios and energy damage indicators of AS-3HT are greater than those of ES-1HT. Early buckling of middle longitudinal bars of Specimen ES-1HT and subsequent loss of confinement are the main reasons behind its relatively less ductile behavior. Specimen ES-1HT with 13% more steel than the ACI 318-89 Code's requirements displayed very poor energy and dissipation characteristics and behaved in a very brittle manner. There was little warning before the failure of the Specimen ES-1HT unlike the Specimen AS-3HT. Better distribution of steel and better lateral support to the longitudinal bars provided tougher response of HSC columns, an effect similar to the one observed for NSC columns (Sheikh and Khoury 1993).

Effect of concrete strength: Three specimens of Configuration A can be compared for the effects of concrete strength. Specimens AS-3HT and AS-5HT have similar $A_{sh}/A_{sh(ACI)}$ and P/P_o values. Specimen AS-17 has different values of these parameters, but the ratios between P/P_o and $A_{sh}/A_{sh(ACI)}$ are approximately equal in three specimens. An examination of the moment-curvature behavior of these specimens and a comparison of ductility parameters indicate that despite the large differences in their concrete strength, all the specimens displayed very similar behavior. Specimen AS-17 was somewhat more ductile compared to the other two specimens when the total behavior up to failure (e.g. $\mu_{\phi 80}$, $N_{\phi t}$, E_t) is considered. From an examination of $\mu_{\phi 90}$, $N_{\phi 80}$, E_{80}, it appears that the higher strength concrete specimens have lower deformability and energy absorbtion capacities initially, but during the later part of the displacement excursions, these properties improve rapidly and the total values are comparable to those of lower strength concrete specimens.

A similar conclusion can be drawn from a comparison of ductility parameters for Specimens ES-13, ES-1HT and ES-8HT shown in Table 2. Their moment-curvature responses are available elsewhere (Bayrak 1995).

CONCLUSIONS

The following conclusions can be drawn from the work reported here.

-As in NSC columns, better distribution of steel in the core and effective lateral support to the longitudinal steel bars improves the deformability and energy dissipation capacity of columns significantly.

-An increase in axial load reduces column's ductility parameters and accelerates stiffness degradation with every load cycle. To compensate for this effect larger amount of confining steel is required.

-Overall behavior of HSC columns was observed to be only slightly less ductile compared with that of NSC columns. However, during the stage of loading immediately beyond peak, the HSC columns displayed significantly lower deformation and dissipation capacities which improved during the later part

of loading excursion. For columns to be comparable, amount of lateral steel should be proportional to the concrete strength and P/P_o should be equal.

-Columns with only four corner bars laterally supported by tie bends and designed according to the current design codes' requirements displayed brittle behavior particularly under large axial loads. Since the code procedure does not consider axial load and steel distribution in the design, the columns such designed can display a wide range of behavior from very ductile to brittle.

ACKNOWLEDGEMENTS

REFERENCES

Bayrak, O. (1995). "High Strength Concrete Columns Subjected to Earthquake Type Loading", M.A.Sc. Thesis, Department of Civil Engineering, University of Toronto, Toronto, 239p.

"Building Code Requirements for Reinforced Concrete" (1989). ACI 318-89, American Concrete Institute, Detroit, Michigan, 351 p.

"Code for the Design of Concrete Structures for Buildings" (1984). CAN3-A23.3M84, Canadian Standards Association, Rexdale, Ontario, 281p.

Sheikh, S.A. and Khoury S.S. (1993). "Confined Concrete Columns with Stubs", ACI Structural Journal, V.90, No.4, July-August 1993, pp. 414-431.
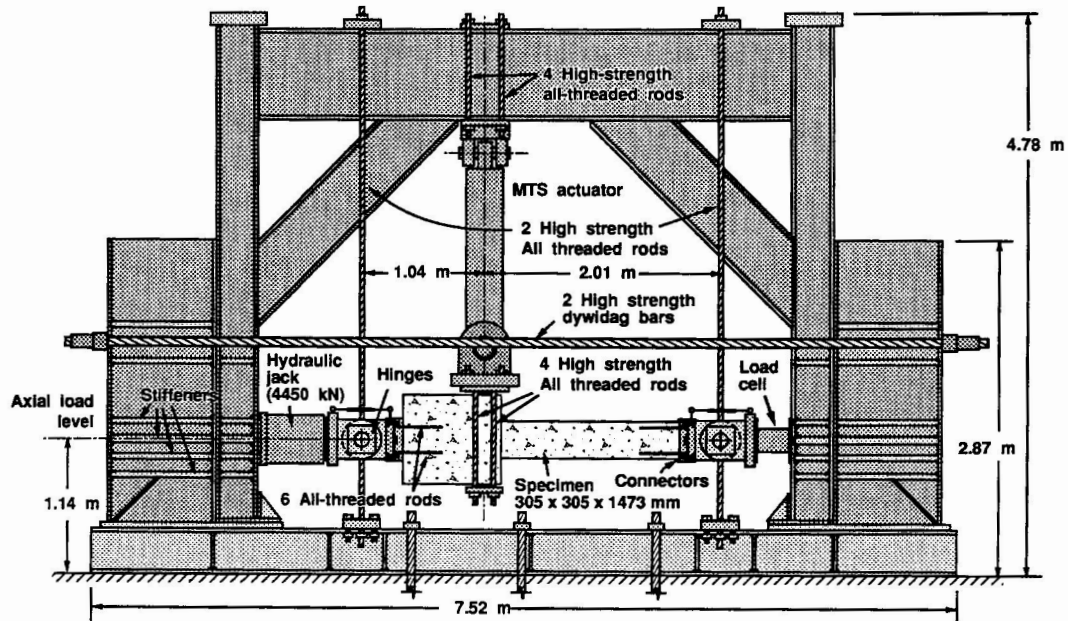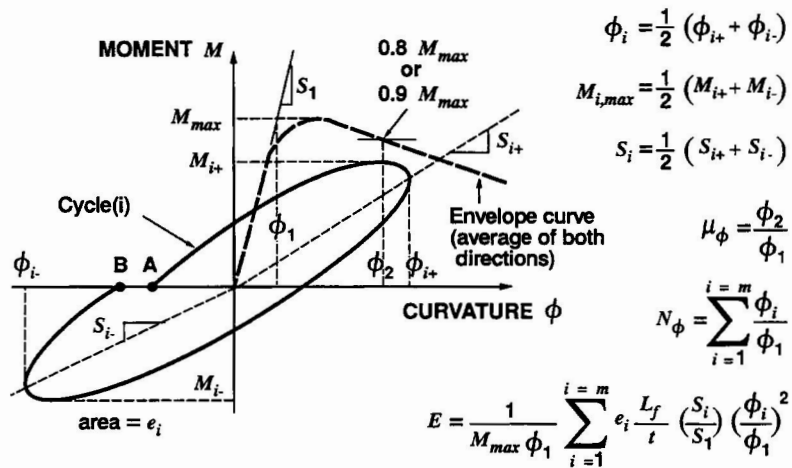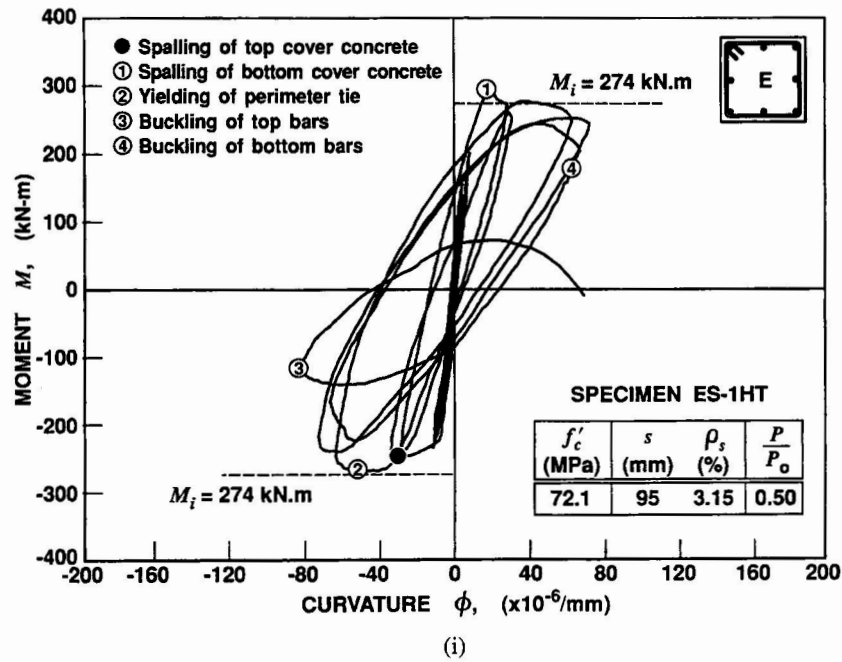
Figure 1. Schematic of Test Setup

$$\phi_i = \frac{1}{2} \left(\phi_{i+} + \phi_{i-} \right)$$

$$M_{i,max} = \frac{1}{2} \left(M_{i+} + M_{i-} \right)$$

$$S_i = \frac{1}{2} \left(S_{i+} + S_{i-} \right)$$

$$\mu_\phi = \frac{\phi_2}{\phi_1}$$

$$N_\phi = \sum_{i=1}^{i=m} \frac{\phi_i}{\phi_1}$$

$$E = \frac{1}{M_{max} \phi_1} \sum_{i=1}^{i=m} e_i \frac{L_f}{t} \left(\frac{S_i}{S_1} \right) \left(\frac{\phi_i}{\phi_1} \right)^2$$

Figure 2. Section Ductility Parameters

(i)

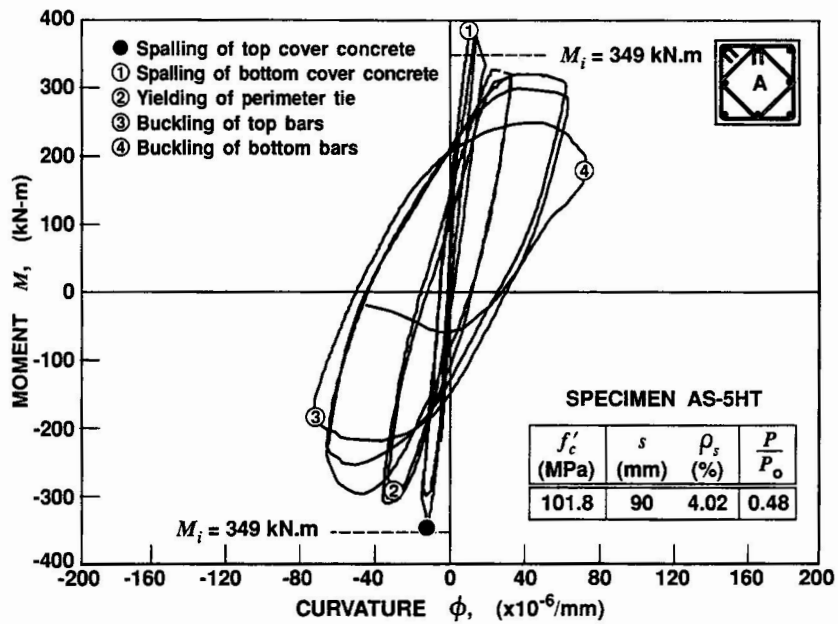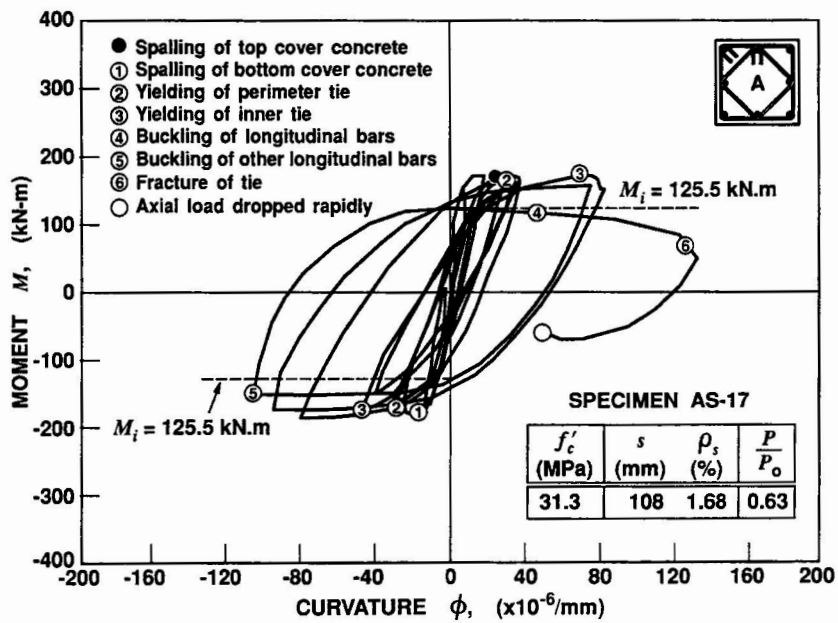Figure 3. Moment - Curvature Response of Specimens
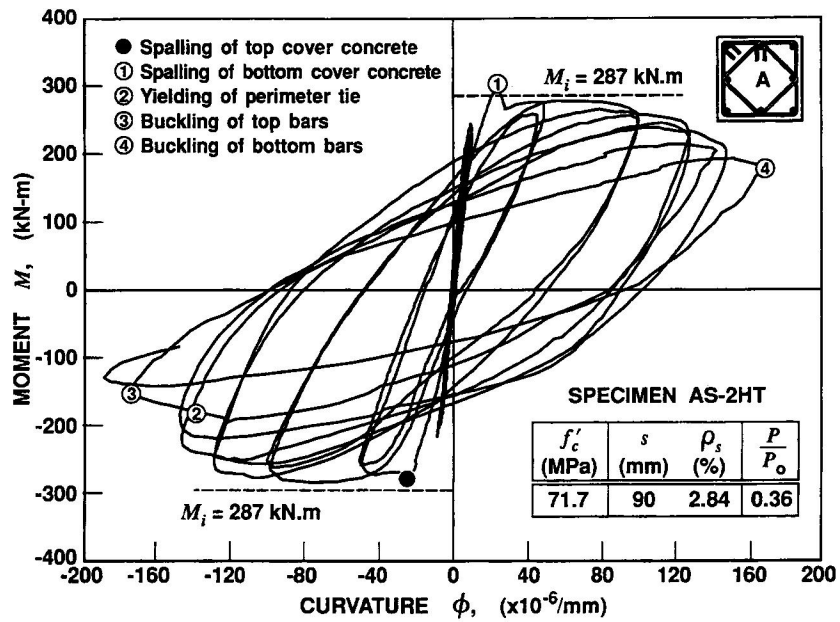
(ii)

(iii)

Figure 3. Moment - Curvature Response of Specimens (cont'd)

483

(iv)

(v)

Figure 3. Moment - Curvature Response of Specimens (cont'd)

484